OTFS: A Potential Waveform for Space–Air–Ground Integrated Networks in 6G and Beyond

OKOYEIGBO, Obinna, DENG, Xutao, IMOIZE, Agbotiname Lucky and SHOBAYO, Olamilekan <http://orcid.org/0000-0001-5889-7082>

telecom

MDPI

Article

OTFS: A Potential Waveform for Space–Air–Ground Integrated Networks in 6G and Beyond

Obinna Okoyeigbo [1,*], Xutao Deng [1], Agbotiname Lucky Imoize [2] and Olamilekan Shobayo [3]

[1] Department of Engineering, Edge Hill University, Ormskirk L39 4QP, UK; dengx@edgehill.ac.uk
[2] Department of Electrical and Electronics Engineering, Faculty of Engineering, University of Lagos, Akoka, Lagos 100213, Nigeria; aimoize@unilag.edu.ng
[3] School of Computing and Digital Technologies, Sheffield Hallam University, Sheffield S1 2NU, UK; o.shobayo@shu.ac.uk
* Correspondence: obinna.okoyeigbo@edgehill.ac.uk

Abstract: 6G is expected to provide ubiquitous connectivity, particularly in remote and inaccessible environments, by integrating satellite and aerial networks with existing terrestrial networks, forming Space–Air–Ground Integrated Networks (SAGINs). These networks, comprising satellites, unmanned aerial vehicles (UAVs), and high-speed terrestrial networks, introduce severe Doppler effects due to high mobility. Traditional modulation techniques like Orthogonal Frequency Division Multiplexing (OFDM) struggle to maintain reliable communication under such conditions. This paper investigates Orthogonal Time Frequency Space (OTFS) modulation as a robust alternative for high-mobility scenarios in SAGINs. Using 6G exploration library in MATLAB, this study compares the bit error rate (BER) performance of OTFS and OFDM under static and multipath channels with varying mobility scenarios from 20 km/h to 2000 km/h, and varying modulation orders (BPSK, QPSK, and 8-PSK). The results indicate that OTFS significantly outperforms OFDM, while maintaining signal integrity under extreme mobility conditions. OTFS modulates information symbols in the delay–Doppler domain, demonstrating a strong robustness against Doppler shifts and delay spreads. This makes it particularly suitable for high-mobility applications such as satellites, UAVs, and high-speed terrestrial networks. Conversely, while OFDM remains effective in static and low-mobility environments, it struggles with severe Doppler effects, common in the proposed SAGINs. These findings reinforce OTFS as a promising modulation technique for SAGINs in 6G and beyond.

Keywords: orthogonal time frequency space (OTFS) modulation; orthogonal frequency division multiplexing (OFDM); delay–Doppler domain; space–air–ground integrated networks (SAGINs); high mobility channels; 6G

Academic Editor: Barbara M. Masini

Received: 29 December 2024
Revised: 17 February 2025
Accepted: 3 March 2025
Published: 11 March 2025

Citation: Okoyeigbo, O.; Deng, X.; Imoize, A.L.; Shobayo, O. OTFS: A Potential Waveform for Space–Air–Ground Integrated Networks in 6G and Beyond. *Telecom* **2025**, *6*, 19. https://doi.org/10.3390/telecom6010019

1. Introduction

The sixth-generation network (6G) is expected to revolutionize the wireless communication industry, by delivering extremely high data rates, ultra-low latency, and massive connectivity beyond previous-generation networks. 6G is expected to provide ubiquitous connectivity, extended coverage, enhanced capacity, and bridge the digital divide by enabling connectivity, even in remote, inaccessible areas and in extreme environments. To achieve these, new technologies like satellite communications and non-terrestrial networks (NTNs) would be deployed to support the already existing terrestrial networks.

The integration of these non-terrestrial (aerial and satellite communication) networks with terrestrial or ground networks gives rise to Space–Air–Ground Integrated Networks

(SAGINs) [1]. Figure 1 shows a simple SAGIN architecture. These networks leverage satellites, unmanned aerial vehicles (UAVs), and drones as relay nodes, providing flexibility and adaptability in communication networks which is unattainable using terrestrial networks only. SAGIN, which is a key enabling technology for 6G, is expected to enable seamless and global coverage, higher data rates, network resilience and reliability due to its multi-layered approach. These will enable applications like autonomous vehicles, high-speed trains, smart cities, drones, and robotics.

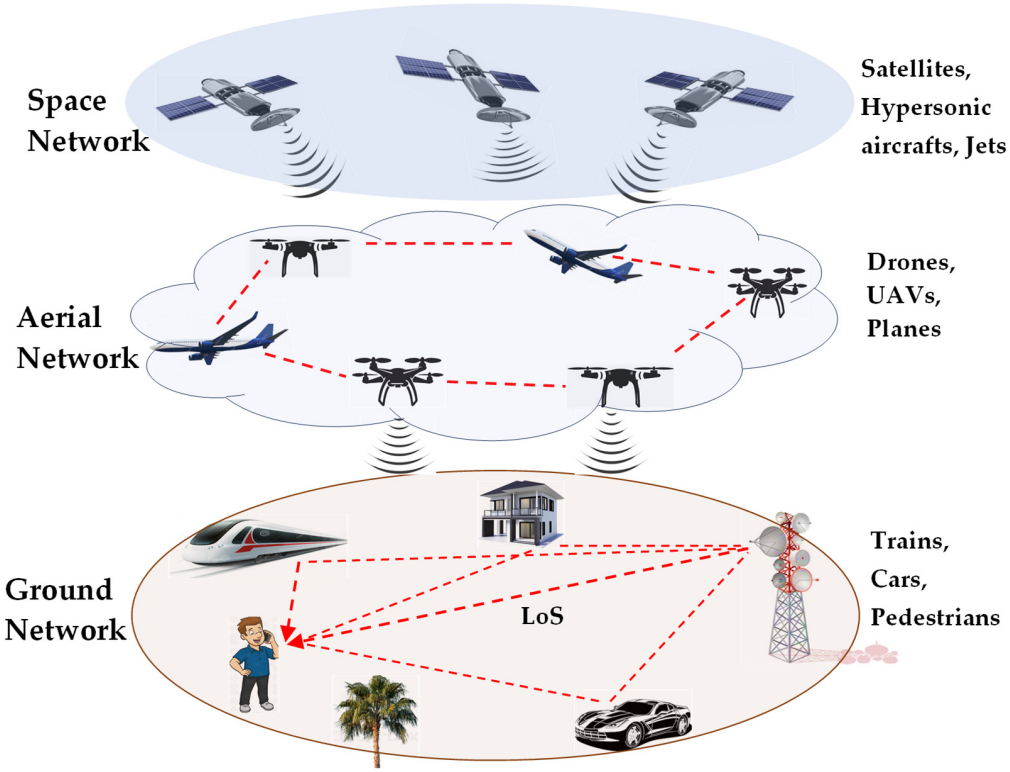

Figure 1. Space–Air–Ground Integrated Network architecture.

The deployment of these new technologies and use cases will present significant challenges. The communication environment in SAGIN is characterized by high mobility of the transceivers or reflectors, multipath propagation due to reflectors in wireless environments, and severe attenuation due to the distance between the transmitter and receiver. These result in the channel varying in frequency and time, with multiple copies of the signal arriving at the receiver at different amplitude, phases, and times, causing the channel to change rapidly due to high mobility and Doppler shift, which is the frequency shift in the received signal due to relative motion between the transmitter and receiver. These introduce severe impairments such as inter-symbol interference (ISI) and inter-carrier interference (ICI), which affect the reliable transmission and reception of signals. Also, 6G is expected to provide Hyper-Reliable and Low-Latency Communication, even in these extreme environments with high mobility and multipath propagation, to enable seamless connectivity in these new applications [2].

Hence, advanced modulation techniques must be employed to address these challenges posed by extreme multipath and high mobility in SAGINs. OTFS and OFDM are two prominent candidates, each with unique characteristics to be explored.

1.1. Orthogonal Frequency Division Multiplexing (OFDM)

Due to its increased spectral efficiency and resilience to multipath fading, OFDM has been the preferred modulation technique for most wireless communication systems,

including 4G, 5G, Wi-Fi, and digital broadcasting standards. OFDM operates in the time–frequency domain. It divides the available bandwidth into multiple orthogonal subcarriers, allowing the parallel transmission of data streams. Therefore, each subcarrier experiences a flat fading channel, making equalization in the frequency domain easier. Therefore, OFDM is highly efficient in frequency-selective fading channels.

However, in high-mobility (time-varying) scenarios, as expected in SAGINs, the performance of OFDM degrades significantly. This is due to the sensitivity of OFDM to time-varying channels with high Doppler effects, leading to inter-carrier interference (ICI). One of the reasons is that the orthogonality between subcarriers, which is crucial for interference-free detection in OFDM, is disrupted by the rapid time-varying nature of the wireless channel [3]. This occurs as Doppler shifts induced by high mobility cause the spectral spreading of the transmitted signals, leading to overlap or interference between adjacent subcarriers, known as inter-carrier interference (ICI) [4].

Another critical issue is the need for frequent transmission of pilot symbols and channel estimation to compensate for the effects of the rapidly changing channel conditions [5]. This results in pilot overhead, which reduces the spectral efficiency of the OFDM scheme in these scenarios. Due to the challenges faced by OFDM in time-varying high-mobility channels, researchers are exploring alternative waveforms like OTFS, to meet the extreme requirements of SAGINs for 6G and beyond.

1.2. Orthogonal Time Frequency Space (OTFS)

OTFS has emerged as an alternative modulation scheme designed to tackle the challenges of multipath and high-mobility scenarios, such as those expected in SAGINs. It is particularly well-suited for doubly selective fading channels (time- and frequency-selective), offering improved robustness compared to traditional modulation schemes. Unlike OFDM, which operates in the time–frequency (TF) domain, OTFS modulates information symbols in the delay–Doppler (DD) domain, where the wireless channel characteristics are more effectively represented and managed [6].

The delay–Doppler domain characterizes the wireless channel based on propagation delay (due to multipaths) and Doppler shift (due to relative motion between transceivers). Unlike the time–frequency domain, where the channel varies rapidly due to time and frequency fluctuations (Figure 2a), the DD domain provides a more structured and stable representation of the channel as shown in Figure 2b.

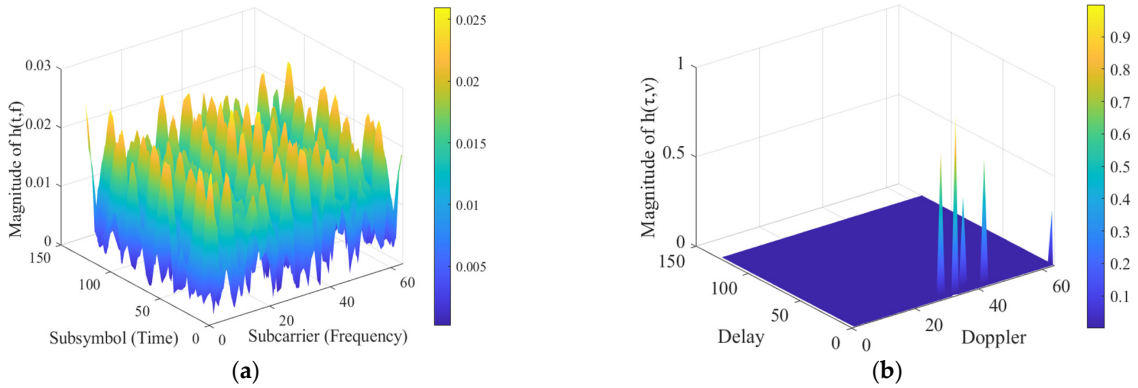

Figure 2. 3D visualization of the wireless channel. (**a**) The TF domain (**b**) The DD domain. This stability arises because channel variations in the DD domain are expressed as discrete delays and Doppler shifts rather than continuous fluctuations. As a result, channel estimation and equalization are simplified. By operating in the DD domain, OTFS inherently aligns with the intrinsic properties of wireless channels, providing resilience against severe Doppler effects. In contrast, in the time–frequency domain, rapid variations in time and frequency create significant challenges for channel estimation.

This capability makes OTFS particularly advantageous for high-mobility scenarios, such as those expected in SAGINs, including satellite communications, UAVs, vehicular networks, and high-speed trains. By effectively mitigating Doppler-induced distortions, OTFS offers significant performance improvements over OFDM, reinforcing its potential for next-generation 6G networks.

1.3. Contribution

This research evaluates and compares the performance of OFDM and OTFS modulation schemes in extreme environments characterized by multiple propagation paths and high mobility, as expected in SAGINs for 6G and beyond. Unlike previous studies that primarily analyze OTFS and OFDM in terrestrial or low-mobility scenarios, this work extends the analysis to highly dynamic SAGIN environments, covering speeds ranging from 20 km/h (V2X, cars) to 2000 km/h (jets and UAVs). Static channels without Doppler effects were also considered.

This research employs 100 GHz carrier frequency and 480 kHz subcarrier spacing, to model THz communication in 6G. By evaluating bit error rate (BER) performance under varying SNR, modulation orders (BPSK, QPSK, and 8-PSK), Doppler shifts, and mobility conditions, this study provides insights into the resilience of OTFS against severe channel impairments. The results highlight OTFS's ability to mitigate Doppler effects and maintain signal integrity, making it a strong candidate for high-mobility 6G applications in SAGINs. These findings contribute valuable insights into the suitability of these modulation techniques for dynamic, high-mobility environments in SAGINs to develop more resilient communication systems for 6G and beyond.

The rest of this research paper is organized as follows. Section 2 comprehensively reviews the related literature on OFDM, OTFS, and SAGIN. Section 3 describes the system model employed in this research. The received signal and channel model are described, along with the principles of OFDM and OTFS modulation and demodulation. Section 4 presents the results and discussion, while Section 5 provides a conclusion and outlines future work.

2. Related Work

Researchers in the past few years have focussed on developing techniques like the OFDM to mitigate the effects of interference in frequency-selective and time-varying channels. In [7], they introduced a space–frequency transmitter diversity technique for frequency-selective fading channels. This technique employs OFDM to transform frequency-selective fading channels into multiple flat fading subchannels, thereby mitigating interference effects.

Lu et al., in [8], presented an ICI mitigation method for OFDM downlinks in high-speed railway (HSR) communication systems with distributed antennas. Multiple carrier frequency offsets cause the ICI due to the number of transmit antennas and the fast time-varying channel in the HSR. Their proposed low-complexity ICI mitigation method achieved almost the same quality of service (QoS) as systems without ICI when the train's velocity was 300 km/h. Furthermore, researchers in [9] have explored index-modulated OFDM (IM-OFDM) with ICI self-cancellation techniques in various communication scenarios, such as underwater acoustic communications and V2X communications. Reference [4] also investigated the performance of IM-OFDM in scenarios with ICI and found that IM-OFDM can exhibit worse performance than conventional OFDM. They proposed a novel ICI self-cancellation technique integrated into the IM-OFDM framework to address this issue. The technique achieves a better trade-off between the ICI cancellation and spectral efficiency of the system [4].

Some researchers have also shown how (Multiple-Input Multiple-Output) MIMO-OFDM can combat interference. In [10,11], MIMO-OFDM channel estimation techniques were proposed to address the interference in time-varying channels. Researchers in [12], discussed the impact of using a cyclic prefix shorter than the channel delay spread in MIMO-OFDM systems. This approach can enhance bandwidth utilization or range extension. However, it can also lead to increased ISI and ICI, which is undesirable.

Overall, these researchers have aimed to improve the performance and reliability of OFDM systems in challenging communication scenarios. However, much improvement still needs to be achieved, and further research is required, especially in channels with very high mobility, as expected in SAGIN.

There has been an increasing research interest in OTFS since 2017, when it was introduced by Hadani et al. [13]. This is because it has shown better BER performance than OFDM in different scenarios, especially in channels with high mobility and Doppler effects. It transforms information carried in the DD domain to the time–frequency domain and exploits the full channel diversity over both time and frequency.

The comparative performance of OFDM and OTFS has been the subject of extensive research. Studies have indicated that while OFDM is highly effective in low-mobility environments, OTFS provides significant gains in high-mobility scenarios. Researchers in [14], highlighted the benefits of OTFS over OFDM. They also derived the explicit input-output relationship, which describes OTFS modulation and demodulation for delay–Doppler channels. Comparisons between OTFS and OFDM have also been conducted to evaluate their pragmatic capacity in scenarios involving non-terrestrial networks (NTN), such as low Earth orbit (LEO) satellite constellations [15].

The application of OTFS modulation in radar systems has also been demonstrated in [16]. An efficient OTFS-based matched filter algorithm was proposed for the estimation of target range and velocity, leveraging the diversity gains for radar processing. OTFS has also been recommended as a modulation technique for millimetre-wave communication systems, offering significant advantages over OFDM in channels with high Doppler effects [17]. MIMO-OTFS has been explored for its high spectral and energy efficiency and has been shown to convert a doubly dispersive channel into an almost non-fading channel in the DD domain through a series of two-dimensional transformations, making it robust to channels with high-Doppler fading [18].

Despite its advantages, OTFS still faces some challenges, particularly in massive MIMO systems, where channel estimation becomes computationally complex due to the large number of antennas at the base station. To address this, researchers in [19] proposed a 3D-structured orthogonal matching pursuit algorithm, improving channel estimation efficiency. Similarly, in [20], a low-complexity message passing (MP) detection algorithm was introduced, leveraging the inherent channel sparsity in large-scale OTFS systems. This MP detection technique enhances OTFS performance in Doppler channels by mitigating inter-Doppler interference (IDI), which arises from fractional Doppler paths misaligned with the Doppler taps.

Further, studies such as [21,22] have explored the broad applications of OTFS in integrated sensing and communication (ISAC), satellite communications, underwater acoustics, and UAV-based networks. While OTFS offers numerous advantages in these domains, the literature also highlights key challenges, including increased computational complexity, hardware implementation difficulties, and integration with ISAC systems.

The concept of Space–Air–Ground Integrated Networks (SAGINs) has also gained significant attention as an enabler for 6G due to its potential to support diverse applications and use cases seamlessly and efficiently. The potential of OTFS technology in improving the performance of SAGINs, particularly in high-Doppler scenarios, has been investigated.

OTFS has been proposed as a modulation technique for Reconfigurable Intelligent Surface (RIS)-assisted SAGIN systems, transforming time-varying channels in the TF domain to time-invariant channels in the DD domain. The study showed that OTFS-based RIS-assisted SAGINs outperform the OFDM alternative in doubly selective high-Doppler scenarios [23]. Furthermore, OTFS has been demonstrated to be resilient to channel-induced Doppler shifts in high-mobility and extreme wireless environments, making it a promising technology for future communication networks [21].

Overall, the literature surrounding OTFS modulation demonstrates its versatility and potential for improving the performance of communication systems in various challenging scenarios. Further research is required to fully explore the potential of OTFS in SAGINs for 6G and beyond, and this paper seeks to address that.

3. System Model

The system model employed in this study aims to accurately simulate the challenging propagation environments encountered in SAGINs. These environments are characterized by fluctuations in received signal strength, delay, and Doppler effects due to multipath propagation and high mobility, such as those encountered in vehicular communications, high-speed trains, unmanned aerial vehicles (UAVs), and non-terrestrial networks (NTNs), as shown earlier.

3.1. Received Signal and Channel Model

Consider a static multipath wireless channel shown in Figure 3a. In this scenario, there is no Doppler effect on the transmitted signal because there is no mobility in the system. However, due to the difference in the propagation delay between the line of sight (LoS) path and reflected paths, multiple copies of the signal s(t) arrive at the receiver at different times. Hence, the received signal $\mathrm{y}(t)$ can be given by [6]:

$$\mathrm{y}(t) = g_1 s(t - \tau_1) + g_2 s(t - \tau_2) \tag{1}$$

where r is the distance, $\tau_1 = r_1/c$ is the LoS path delay, $\tau_2 = (r_2 + r_3)/c$ is the reflected path delay, and c is the speed of light ($3 \times 10^8 \mathrm{m/s}$). The difference between the maximum and minimum propagation delays ($\tau_{\max} - \tau_{\min}$) gives the delay spread.

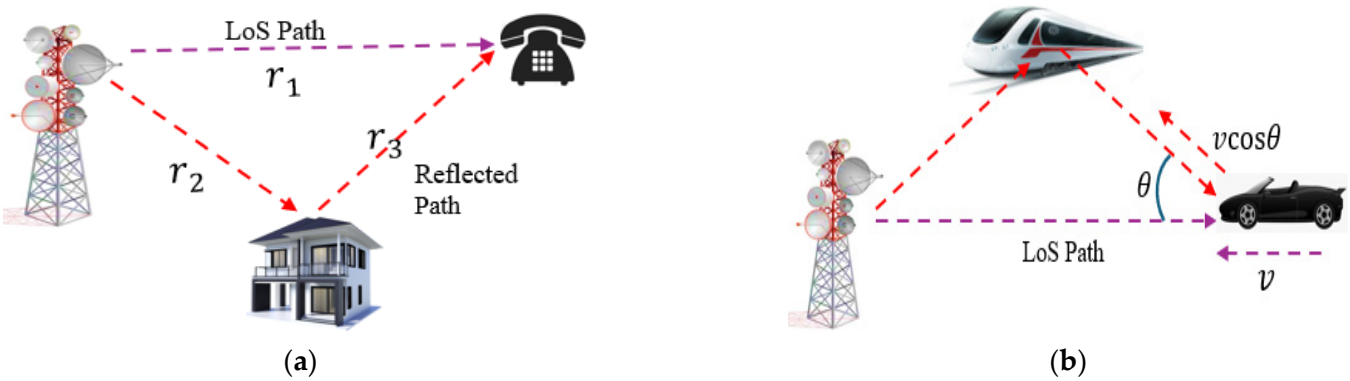

Figure 3. Wireless channel scenarios. (**a**) Static multipath channel with different propagation delay. (**b**) Multipath channel with Doppler effects due to mobility and different angles of arrival [6].

Consider another scenario where there is mobility between the transmitter, receiver, or reflectors in the environment, with a velocity v, as shown in Figure 3b. The Doppler shift due to a relative velocity ν can be expressed as $\frac{v}{c} f_c$. Hence, the received signal is given

as the sum of the different copies of the transmitted signal, which is delayed and Doppler shifted as shown [6]:

$$y(t) = \underbrace{g_1 e^{j2\pi\nu_1(t-\tau_1)}}_{g(\tau_1,t)} s(t-\tau_1) + \underbrace{g_2 e^{j2\pi\nu_2(t-\tau_2)}}_{g(\tau_2,t)} s(t-\tau_2) \tag{2}$$

where $g(\tau_i, t) = g_i e^{j2\pi\nu_i(t-\tau_i)}, i = 1, 2$, is the time-varying attenuation due to channel effects, $\nu_1 = \frac{v}{c} f_c$, and $\nu_2 = \frac{v\cos\theta}{c} f_c$ represents the Doppler shift of the direct LoS path and reflected path, respectively, and $|\nu_2 - \nu_1|$ is the Doppler spread.

The received signal can, therefore, be represented by

$$y(t) = \int_0^\infty g(\tau, t) s(t-\tau) d\tau \tag{3}$$

where $g(\tau, t)$ is the channel impulse response, which is a function of time t and delay τ.

Taking the Fourier transform of the delay–time channel impulse response $g(\tau, t)$ along the delay domain gives the time–frequency channel impulse response at the time t as shown:

$$H(f, t) = \int_\tau g(\tau, t) e^{-j2\pi f\tau} d\tau \tag{4}$$

If the channel has multiple propagation paths P, and the time-varying attenuation is given by $g(\tau_i, t) = g_i e^{j2\pi\nu_i(t-\tau_i)}, i = 1, 2$, then the frequency response of the channel can be given as

$$H(f, t) = \sum_{i=1}^{P} g_i e^{-j2\pi\nu\tau_i} e^{-j2\pi(f\tau_i - \nu_i t)} \tag{5}$$

where $H(f, t)$ is assumed to be slowly time-varying. Hence, when the channel is static, and $\nu_i = 0$, then the channel becomes time-independent $H(f)$.

Therefore, due to the limited number of channel paths P, the sparse representation of the channel in the DD domain is given by

$$h(\tau, \nu) = \sum_{i=1}^{P} g_i e^{-j2\pi\nu_i\tau_i} \delta(\tau - \tau_i)\delta(\nu - \nu_i) \tag{6}$$

If the constant phase shift $e^{-j2\pi\nu_i\tau_i}$ is absorbed into the channel coefficient g_i, then the wireless channel in the DD domain can be completely represented by the parameters (g_i, τ_i, ν_i), for $i = 1, \ldots, P$ as shown:

$$h(\tau, \nu) = \sum_{i=1}^{P} g_i \delta(\tau - \tau_i)\delta(\nu - \nu_i) \tag{7}$$

Hence, the received signal given in (2) can therefore be expressed as

$$y(t) = \sum_{i=1}^{P} g_i e^{j2\pi\nu_i(t-\tau_i)} s(t - \tau_i) \tag{8}$$

which is the summation of the different copies of the transmitted signal, which are delayed and Doppler-shifted.

Therefore, for a multipath time-varying channel (or a doubly dispersive channel), the received signal $y(t)$ can be given by the following expressions:

$$y(t) = \int_\tau g(\tau, t) s(t-\tau) d\tau \tag{9}$$

$$= \int_f H(f,t)S(f)e^{j2\pi ft}df \tag{10}$$

$$= \int_\nu \int_\tau h(\tau,\nu)s(t-\tau)e^{j2\pi\nu t}d\tau d\nu \tag{11}$$

where $S(f)$ represents the Fourier transform of the transmitted signal $s(t)$ in the time domain, $g(\tau,t)$ represents the time-varying (or delay–time) channel impulse response, $H(f,t)$ represents the channel in the time–frequency domain as represented in an OFDM system and $h(\tau,\nu)$ represents the channel in the delay–Doppler domain as given in an OTFS system.

Using a pair of two-dimensional Symplectic Fourier transforms (SFTs) and Inverse Symplectic Fourier Transforms (ISFTs), the channel can be transformed between the TF domain $H(f,t)$ and the DD domain $h(\tau,\nu)$, as shown in the following equations:

$$h(\tau,\nu) = \text{SFT}\{H(f,t)\} = \iint H(f,t)e^{-j2\pi(\nu t - f\tau)}dtdf \tag{12}$$

$$H(f,t) = \text{ISFT}\{h(\tau,\nu)\} = \iint h(\tau,\nu)e^{j2\pi(\nu t - f\tau)}d\tau d\nu \tag{13}$$

Similarly, the information-carrying symbols can be transformed from the time–frequency domain to the DD domain and vice versa using the SFFT and the ISFFT, respectively.

3.2. OTFS Modulation and Demodulation

At the transmitter, information symbols $X[k,l]$ are initially mapped onto an $M \times N$ two-dimensional DD transmit data grid $x_{dd}[k,l]$, where k and l are the discrete delay and Doppler axis indices, $k = 0,1,\ldots,M-1$ and $l = 0,1,\ldots,N-1$, respectively. The grid represents one OTFS symbol, and each column of the grid is a sub-symbol [24].

Hence, k and l can be referred to as the normalized delay and Doppler shifts, while the actual discretized delay (τ_k) and Doppler shift (ν_l) are given by

$$\tau_k = \frac{k}{M\Delta f},\ k = 0,1,\ldots,M-1 \tag{14}$$

$$\nu_l = \frac{l}{NT},\ l = 0,1,\ldots,N-1 \tag{15}$$

where Δf is the subcarrier spacing in Hertz and T is the OTFS sub-symbol duration in seconds (plus the cyclic prefix, if any). These symbols are then transformed into the TF domain using the ISFFT, facilitating transmission over the wireless channel. The received signal is converted back to the DD domain at the receiver using the SFFT, enabling effective demodulation and decoding of the transmitted information.

The discrete channel response $H[m,n]$ can be derived from the continuous channel $h(\tau,\nu)$ using the relationship $t = nT$ and $f = m\Delta f$ as shown:

$$H[m,n] = \iint h(\tau,\nu)e^{j2\pi(\nu nT - m\Delta f\tau)}d\tau d\nu \tag{16}$$

For a discrete channel with P paths, the DD domain channel is given by

$$h[k,l] = \sum_{i=1}^{P} g_i\delta(k-k_i)\delta(l-l_i) \tag{17}$$

and the discrete ISFT transforms this DD domain channel $h[k,l]$ into the discrete TF domain channel $H[m,n]$ as follows:

$$H[m,n] = \frac{1}{\sqrt{MN}} \sum_{k=0}^{M-1} \sum_{l=0}^{N-1} h[k,l] e^{(j2\pi(\frac{nl}{N} - \frac{mk}{M}))} \tag{18}$$

The process of OTFS modulation and demodulation can be performed on an existing OFDM system, where M corresponds to the number of subcarriers (in an OFDM symbol) and N the number of OFDM symbols contained in a single frame. Figure 4 shows the relationship between OTFS and OFDM systems in the DD and TF domains, respectively.

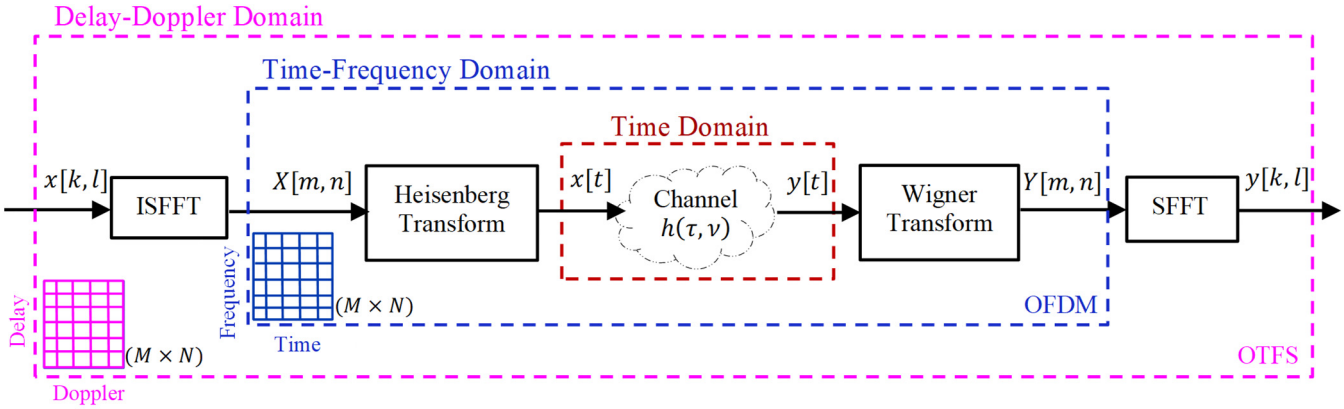

Figure 4. OTFS modulation and demodulation block diagram.

Hence, to convert modulated symbols from the delay–Doppler domain $x_{dd}[k,l]$ to the time–frequency domain $X_{tf}[m,n]$, the ISFFT is employed as shown [13]:

$$X_{tf}[m,n] = \frac{1}{\sqrt{MN}} \sum_{k=0}^{M-1} \sum_{l=0}^{N-1} x_{dd}[k,l] e^{(j2\pi(\frac{nl}{N} - \frac{mk}{M}))} \tag{19}$$

where m and n denote the frequency and time indices, respectively.

The ISFFT can be decomposed into two steps. First, an inverse Discrete Fourier Transform (IDFT) is applied to the transpose of $x_{dd}\left(x_{dd}^T\right)$, which operates along the Doppler axis and transforms x_{dd} from the DD domain to the delay–time domain X_{dt}, and then the result is transposed back to the proper array dimension as shown:

$$X_{dt}[k,n] = \frac{1}{\sqrt{N}} \sum_{l=0}^{N-1} x_{dd}[k,l] e^{j\frac{2\pi nl}{N}} = IFFT\left(x_{dd}^T\right)^T \tag{20}$$

Then, a Discrete Fourier Transform (DFT) is applied along the delay axis of X_{dt}, to obtain the TF domain representation as shown:

$$X_{tf}[m,n] = \frac{1}{\sqrt{M}} \sum_{k=0}^{M-1} X_{dt}[k,n] e^{-j\frac{2\pi mk}{M}} = FFT(X_{dt}) \tag{21}$$

Combining (20) and (21), the ISFFT can be simplified and implemented as

$$X_{tf}[m,n] = FFT\left(IFFT\left(x_{dd}^T\right)^T\right) \tag{22}$$

The time–frequency domain signal $X_{tf}[m,n]$, can now be converted to a time-domain signal $x(t)$ using the Heisenberg transform (equivalent to an OFDM modulator) as shown:

$$x(t) = \sum_{n=0}^{N-1} \sum_{m=0}^{M-1} X_{tf}[m,n] g(t-nT) e^{j2\pi m\Delta f(t-nT)} \tag{23}$$

where T is the duration of the OFDM symbol (plus cyclic prefix if any) and $g(t)$ is the pulse-shaping filter.

The pulse-shaping filter aims to mitigate the channel spreading caused by fractional Doppler shifts (when the Doppler frequency does not fall on a multiple of $1/(NT)$). Suppose the filter is a rectangular window time-limited to 0 to T, then the Heisenberg transform becomes an OFDM modulator operating over each column of the signal X_{tf}. This, therefore, reduces the OTFS modulator to a two-dimensional ISFFT-precoded OFDM modulator. Where the 2D ISFFT transforms the Doppler domain to the time domain using IDFT and the delay domain to the frequency domain using the DFT. Finally, the Heisenberg transform converts the TF domain to the time domain using the IDFT.

The signal $x(t)$ is transmitted through a high-mobility channel with delay–Doppler channel impulse response $h(\tau,\nu)$, which is equivalent to the delay-time channel response given by $g(\tau,\mathrm{t})$, where τ and ν represents the delay and Doppler shift, respectively, and $z(t)$ represents noise. Therefore, the received signal $y(t)$ is expressed as

$$y(t) = \int_{\nu} \int_{\tau} h(\tau,\nu) e^{j2\pi\nu(t-\tau)} x(t-\tau) d\tau d\nu + z(t) \tag{24}$$

At the receiver, the received signal $y(t)$ in the time domain is converted to TF domain using the Wigner transform, equivalent to the OFDM demodulator, as shown:

$$Y_{tf}[m,n] = \int_{\tau} y(\mathrm{t}) g_{rx}^{*}(t-nT) e^{-j2\pi m\Delta f(t-nT)} dt \tag{25}$$

and the TF domain signal is then converted back to the DD domain using the SFFT as shown:

$$y_{dd}[k,l] = \frac{1}{\sqrt{MN}} \sum_{m=0}^{M-1} \sum_{n=0}^{N-1} Y_{tf}[m,n] e^{(-j2\pi(\frac{nl}{N} - \frac{mk}{M}))} \tag{26}$$

effectively recovering the DD domain representation of the transmitted symbols.

OTFS modulation can also be implemented using the inverse Zak transform, which is mathematically equivalent to the combination of ISFFT and the Heisenberg transform [6]. The inverse Zak transform provides an alternative and computationally efficient method for transforming the input signal x_{dd} from the DD domain to the delay–time domain X_{dt}, bypassing the need for the IDFT-DFT pair. Therefore, the input signal x_{dd} can be converted to the delay time domain X_{dt} as shown:

$$X_{dt} = IFFT\left(X_{tf}\right) \tag{27}$$

$$X_{dt} = IFFT\left(FFT\left(IFFT\left(x_{dd}^{T}\right)^{T}\right)\right) \tag{28}$$

$$X_{dt} = IFFT\left(x_{dd}^{T}\right)^{T} \tag{29}$$

where the superscript T denotes the transpose. Note that the IFFT-FFT combination cancels out and reduces the operation to an IFFT across the Doppler axis, thereby reducing the

computational complexity. The intermediate result X_{dt} is the inverse Zak transform, and the time-domain signal x_t is obtained by vectorizing X_{dt} [25].

4. Results and Discussion

This section presents the simulation results of the above system for performance analysis. The system was implemented in the 6G Exploration Library in MATLAB R2024a [26]. To ensure a fair comparison between OFDM and OTFS, identical system parameters are used across both modulation schemes. The simulation parameters, given in Table 1, are carefully selected to reflect realistic operating conditions in SAGINs in 6G, including vehicular communications, high-speed trains, UAVs, and NTNs. A carrier frequency of 100 GHz is chosen to align with the anticipated use of THz spectrum in 6G for high-capacity communication, while a subcarrier spacing of 480 kHz helps mitigate ICI under extreme Doppler shifts [17]. Larger subcarrier spacings are beneficial in such environments as they allow for more bandwidth and reduce the system's sensitivity to frequency dispersion.

Table 1. Simulation Parameters.

Parameter	Value
Number of Subcarriers (M)	128
Number of Sub-symbols per Frame (N)	64
Subcarrier Spacing	480 kHz
Carrier Frequency	100 GHz
Padding Length	10 samples
Signal-to-Noise Ratio (SNR dB)	30 dB
Mobility Scenarios and Application	20–120 km/h (Cars, V2X, trains) 300–500 km/h (High Speed Trains and UAVs) 1000–2000 km/h (Jets)
Modulation Order	BPSK, QPSK, 8-PSK
Channel Estimation Method	Linear MMSE

The Doppler ranges considered (20–2000 km/h) correspond to a variety of real-world mobility scenarios, from vehicular networks (V2X) to high-speed aerial platforms, ensuring our results are applicable to a broad spectrum of mobility conditions. The number of subcarriers (M = 128) and sub-symbols per frame (N = 64) are selected to provide a balance between computational complexity and resolution in the delay–Doppler domain. The Linear MMSE channel estimation method is employed due to its effectiveness in mitigating channel impairments in high-mobility environments. These choices ensure that our results are both theoretically sound and practically relevant for future 6G deployments.

4.1. Channels with No Doppler Effects

The simulated scenario in Figure 5 describes an ideal wireless channel with a single line of sight (LoS) path between a fixed transmitter and receiver. There is no mobility, hence there is no Doppler shift. The channel is constant over time, indicating a stationary environment. This is an ideal condition, suitable for experimental purposes and a benchmark for theoretical analysis. Figure 5 compares the BER performance of OTFS and OFDM for different modulation orders (BPSK, QPSK, and 8-PSK). It is observed that both OFDM and OTFS give a very good performance because the subcarriers experience a stable channel, and there is no ISI or ICI. However, OTFS slightly outperforms OFDM for all SNR ranges. This can be attributed to the fact that OTFS operates in the delay–Doppler domain and captures the full time–frequency diversity of the channel, even in simple LoS scenarios. On the other hand, OFDM modulates signals in the frequency domain and may suffer from small imperfections like frequency offset between transmitter and receiver.

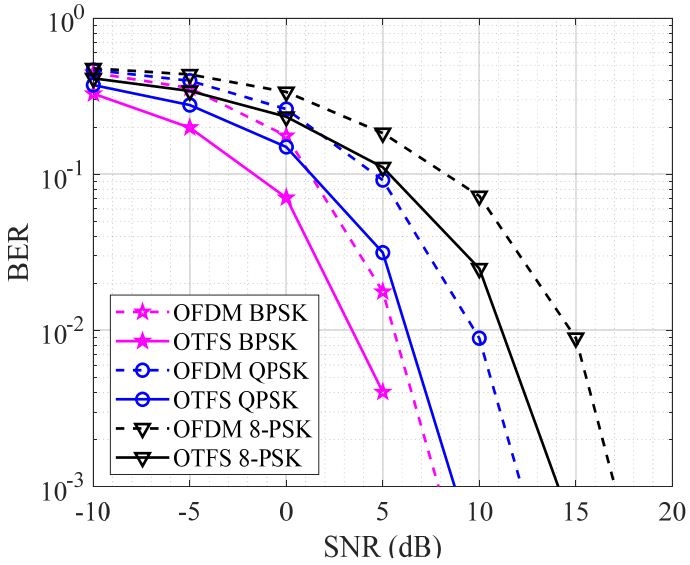

Figure 5. BER performance comparison of OTFS and OFDM in a LoS channel with different modulation orders.

Figure 6 describes a static multipath channel with no mobility and, hence, no Doppler shift. The channel characteristics do not change over time, which indicates a stationary environment. This channel type is often encountered in indoor environments or fixed wireless links with multiple propagation paths, where the transmitter and receiver are relatively stationary. These multiple propagation paths can lead to the distortion of the signal in the frequency domain.

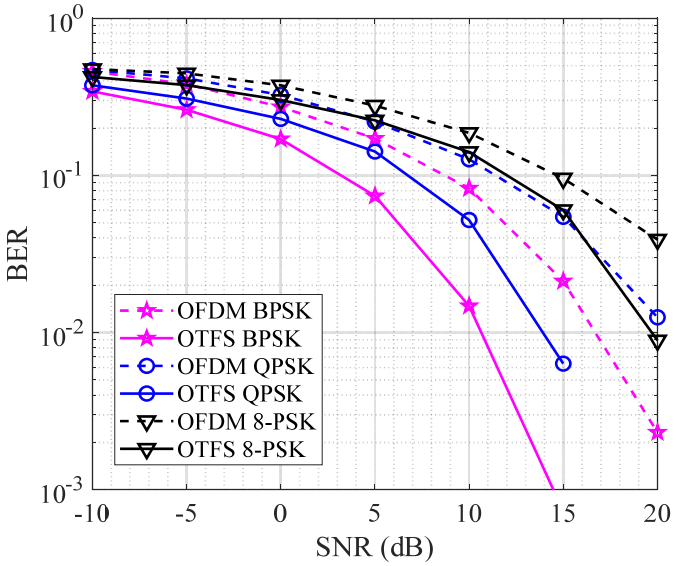

Figure 6. BER performance comparison of OTFS and OFDM in a static multipath channel for different modulation orders.

In Figure 6, the BER performance of OTFS and OFDM is compared for different modulation orders (BPSK, QPSK, and 8-PSK) in a static multipath channel. OFDM performs well in a static multipath channel because it converts a frequency-selective wideband channel into multiple flat-fading narrowband subcarriers. This allows the system to deal with frequency selectivity more easily since each subcarrier experiences a flat-fading channel.

OTFS is also designed to perform well in multipath channels by transforming the time–frequency selective fading into the delay–Doppler domain, where it can better capture

the channel's multipath structure and spread symbols over time and frequency resources. OTFS also spreads the symbols over time and frequency, which helps mitigate ISI and ensures that multipath components are combined constructively, leading to better detection. This provides better diversity gains compared to OFDM in a multipath environment. OTFS shows better BER performance than OFDM because of its ability to spread information across the entire time–frequency grid and exploit multipath diversity more effectively.

4.2. Channels with Doppler Effects

This section analyses multipath channels under varying levels of mobility, ranging from low speeds (20 km/h) to extreme speeds (2000 km/h). As mobility increases, the Doppler effect becomes more pronounced, leading to time-varying frequency selectivity and ICI. These effects significantly impact the BER performance, making it crucial to evaluate their robustness under different mobility conditions.

Figure 7 shows the BER vs. SNR performance of OTFS and OFDM in multipath channels with mobility ranging from 20 to 120 km/h. This is a low-to-moderate mobility scenario, as seen in vehicular communications, drones, and trains in terrestrial networks.

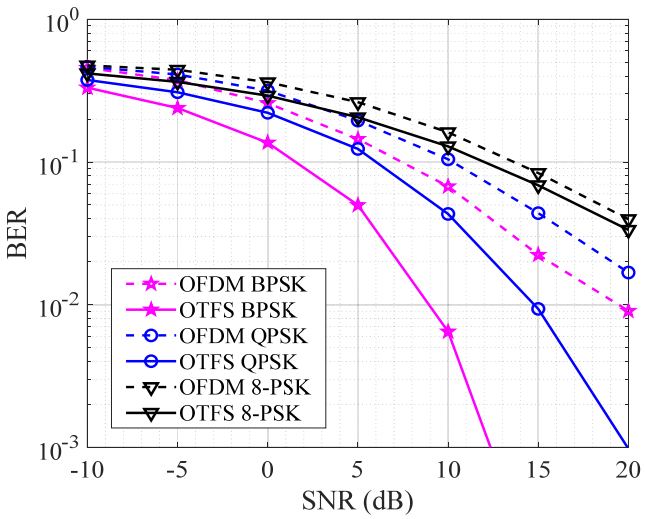

Figure 7. BER performance comparison of OTFS and OFDM in a multipath channel with different modulation orders and mobility ranging from 20 to 120 km/h.

It is observed that OFDM performs relatively well in these scenarios, as the effects of ICI caused by Doppler shifts are not significant at these moderate speeds. OFDM is still able to maintain reliable communication with minimal BER degradation, making it suitable for low-to-moderate mobility scenarios.

OTFS also demonstrates good performance in these low to moderate mobility scenarios. However, the advantages of OTFS are not significant in low-mobility scenarios because the delay–Doppler domain advantages, which OTFS thrives on, are limited when the Doppler effects are less severe.

At lower modulation orders (BPSK and QPSK), OTFS achieves a lower BER than OFDM, highlighting its robustness against interference. However, at higher-order modulations (8-PSK), both OTFS and OFDM exhibit similar BER performance, because higher-order constellations are inherently more sensitive to noise and interference.

Figure 8 presents the BER vs. SNR performance of OTFS and OFDM in multipath channels under moderate-to-high mobility conditions (300–500 km/h), typically experienced in high-speed trains and aerial platforms such as high-speed UAVs.

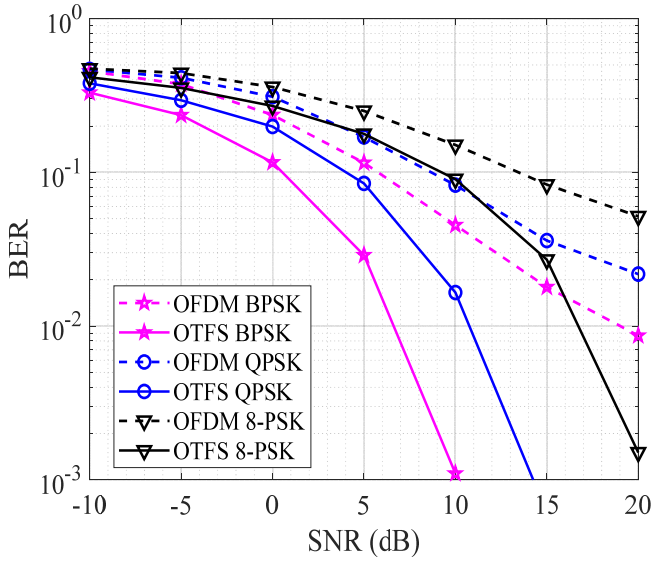

Figure 8. BER performance comparison of OTFS and OFDM in a multipath channel with different modulation orders and high mobility ranging from 300 to 500 km/h.

At these higher mobility levels, Doppler effects become significant, leading to time-varying frequency selectivity and introducing ICI. This results in degradation of the BER performance, particularly at higher SNR values, where the BER curve begins to plateau. OFDM, which is designed for time-invariant or slow-fading channels, fails to track rapid channel variations in high-mobility conditions, making it unsuitable for such scenarios.

OTFS, on the other hand, effectively handles Doppler spread by operating in the delay–Doppler domain, maintaining a much lower BER compared to OFDM. Even under high-mobility conditions, OTFS achieves a BER of 10^{-3} at an SNR of approximately 10 dB with BPSK modulation. Unlike OFDM, OTFS maintains consistent performance as mobility increases, demonstrating strong resilience to Doppler shifts and multipath effects, allowing it to sustain lower BER at higher speeds.

Figure 9 presents the BER vs. SNR performance of OTFS and OFDM in multipath channels, comparing different modulation orders (BPSK, QPSK, and 8-PSK) under extreme mobility scenarios at speeds between 1000 km/h and 2000 km/h. These conditions are representative of high-speed NTNs such as military jets and supersonic aircrafts.

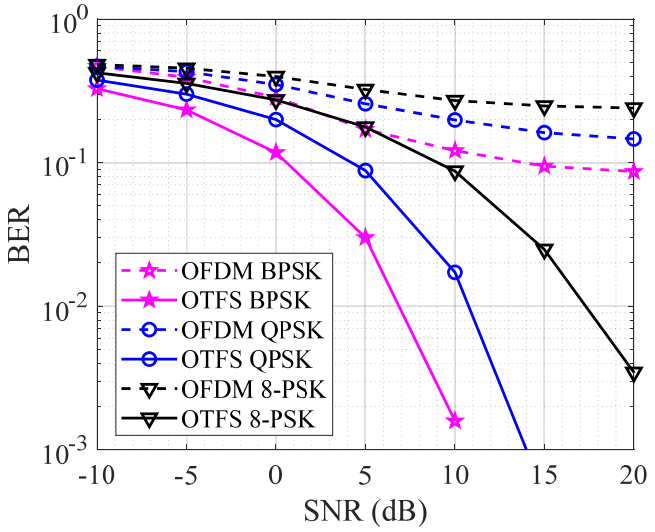

Figure 9. BER performance comparison of OTFS and OFDM in a multipath channel with different modulation orders in extreme mobility scenarios (1000 km/h to 2000 km/h).

At these extreme mobility conditions, OFDM experiences severe Doppler effects, leading to significant ICI and poor BER performance, due to time-varying frequency selectivity. As the modulation order increases (from BPSK to 8-PSK), the BER worsens because higher-order modulations are more susceptible to noise and interference. The BER curves for OFDM tend to flatten out, indicating that increasing SNR does not significantly improve performance, making OFDM unsuitable for such extreme mobility conditions.

In contrast, OTFS consistently outperforms OFDM across all modulation schemes. It effectively mitigates Doppler and multipath effects, resulting in significantly lower BER. Unlike OFDM, the BER of OTFS continues to decrease with increasing SNR, demonstrating its robustness in extreme mobility scenarios. This is because OTFS operates in the delay–Doppler domain, spreading symbols across both time and frequency. This efficiently manages the time and frequency domain distortions, offering resilience against mobility-induced ICI. OTFS also benefits from more accurate channel estimation in high-mobility environments. By leveraging the delay–Doppler representation, OTFS enables effective pilot symbol utilization and a structured channel matrix, simplifying equalization and improving the BER performance.

Figure 10 shows the BER vs. SNR performance of OTFS and OFDM in multipath channels under varying mobility conditions (20 km/h, 400 km/h, and 2000 km/h). This provides a clear comparison of how increasing mobility affects both modulation schemes.

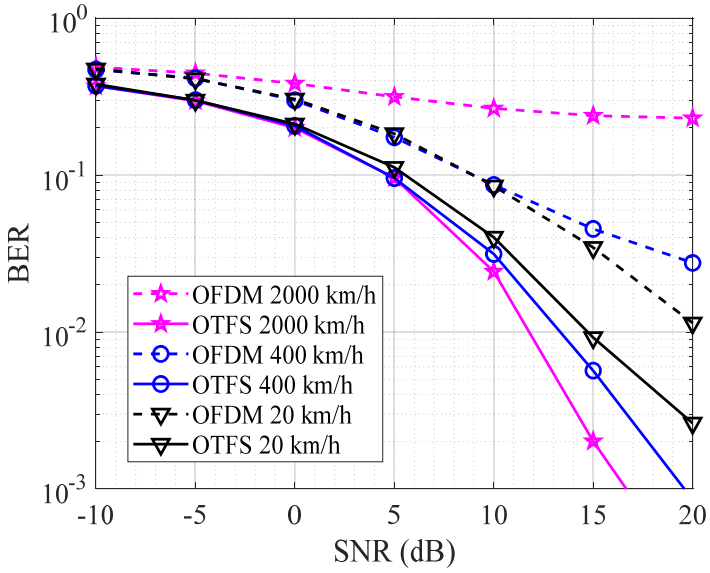

Figure 10. BER performance comparison of OTFS and OFDM in a multipath channel under different mobility scenarios (20 km/h, 400 km/h, and 2000 km/h).

As mobility increases from 20 km/h to 2000 km/h, the BER of OFDM degrades significantly. While OFDM performs well at low mobility (20 km/h), where the BER decreases with increasing SNR, its performance deteriorates at higher mobility (2000 km/h). At SNR values beyond 15 dB (at 2000 km/h), the BER curve flattens out, indicating that OFDM struggles with ISI and ICI caused by high Doppler effects.

In contrast, OTFS consistently outperforms OFDM across all mobility conditions. The BER curve for OTFS continues to decrease as SNR increases, achieving a BER of 10^{-3} at approximately 20 dB SNR. It is also observed that OTFS shows improved performance as mobility increases (from 20 to 2000 km/h), demonstrating that it thrives in high-mobility environments. This behaviour is attributed to OTFS's delay–Doppler domain processing, which effectively mitigates Doppler spread and multipath fading.

5. Conclusions

The performance of OTFS and OFDM was evaluated under various mobility scenarios expected in SAGINs. The results demonstrate that OTFS outperforms OFDM in high-mobility and multipath environments, which are characteristic of SAGINs. While OFDM remains effective in static and low-mobility channels, it struggles to mitigate severe Doppler effects and multipath fading encountered in high-mobility scenarios. OTFS, by operating in the delay–Doppler domain, enables superior channel estimation, improved equalization, and greater resilience to ICI and multipath effects. This results in significantly lower BER and more reliable communication in dynamic environments.

Despite these advantages, OTFS introduces higher computational complexity, which may impact its practical deployment in 6G networks. Nevertheless, given the growing demand for reliable, high-mobility communication, OTFS emerges as a strong candidate for SAGINs in 6G and beyond, enabling seamless integration across space, air, and ground network layers.

Future work may focus on evaluating the practical challenges of OTFS implementation, including computational complexity and hardware feasibility. Additionally, further research could explore the integration of OTFS with MIMO and massive MIMO systems to enhance spectral efficiency and capacity. Another promising direction is the application of deep learning-based techniques for channel estimation and equalization to further improve the performance of OTFS in dynamic channels. These investigations will provide deeper insights into the viability of OTFS for SAGINs and its potential role in 6G and beyond.

Author Contributions: Conceptualization, O.O.; methodology, O.O.; software, O.O. and X.D.; validation, O.O., X.D. and A.L.I.; formal analysis, O.O. and O.S.; investigation, O.O.; resources, O.O.; writing—original draft preparation, O.O.; writing—review and editing, O.O., O.S. and A.L.I.; supervision, X.D.; project administration, X.D. All authors have read and agreed to the published version of the manuscript.

Funding: This research received no external funding.

Data Availability Statement: The data that support the findings of this study are available from the corresponding author upon reasonable request.

Conflicts of Interest: The authors declare no conflicts of interest.

References

1. Liu, J.; Shi, Y.; Kato, N. Space-Air-Ground Integrated Network: A Survey. *IEEE Commun. Surv. Tutor.* **2018**, *20*, 2714–2741. [CrossRef]
2. Geraci, G.; Garcia-Rodriguez, A.; Azari, M.M.; Lozano, A.; Mezzavilla, M.; Chatzinotas, S.; Chen, Y.; Rangan, S.; Di Renzo, M. What Will the Future of UAV Cellular Communications Be? A Flight From 5G to 6G. *IEEE Commun. Surv. Tutor.* **2022**, *24*, 1304–1335. [CrossRef]
3. Wang, T.; Proakis, J.G.; Masry, E.; Zeidler, J.R. Performance degradation of OFDM systems due to doppler spreading. *IEEE Trans. Wirel. Commun.* **2006**, *5*, 1422–1432. [CrossRef]
4. Li, Y.; Wen, M.; Cheng, X.; Yang, L.Q. Index modulated OFDM with ICI self-cancellation. In Proceedings of the 2016 International Conference on Computing, Networking and Communications (ICNC), Kauai, HI, USA, 15–18 February 2016. [CrossRef]
5. Geetha, C.; Vanitha, M.; Parimala, A.; Kalaiarasi, D. A Novel Channel Estimation Scheme for MIMO-OFDM Systems based on CDD. In Proceedings of the 5th International Conference on Inventive Computation Technologies, ICICT 2022—Proceedings, Lalitpur, Nepal, 20–22 July 2022; pp. 747–753. [CrossRef]
6. Hong, Y.; Thaj, T.; Viterbo, E. *Delay-Doppler Communications*; Elsevier: Amsterdam, The Netherlands, 2022. [CrossRef]
7. Lee, K.F.; Williams, D.B. A space-frequency transmitter diversity technique for OFDM systems. In Proceedings of the Globecom'00—IEEE. Global Telecommunications Conference—Conference Record (Cat. No. 00CH37137), San Francisco, CA, USA, 27 November–1 December 2000; pp. 1473–1477. [CrossRef]

8. Lu, J.; Chen, X.; Liu, S.; Fan, P. Location-Aware Low Complexity ICI Reduction in OFDM Downlinks for High-Speed Railway Communication Systems with Distributed Antennas. In Proceedings of the 2016 IEEE 83rd Vehicular Technology Conference (VTC Spring), Nanjing, China, 15–18 May 2016; pp. 1–5. [CrossRef]
9. Kaur, N.; Kumar, N. Comparative Analysis of ICI Self Cancellation Techniques for Wavelet OFDM Under Different Channels in Simulink. *Wirel. Pers. Commun.* **2019**, *105*, 1513–1525. [CrossRef]
10. Idris, A.; Sabry, M.; Razak, N.I.A.; Yusof, A.L.; Mara Shah Alam, U. Fast Time-Varying Channels in MIMO-OFDM System Using Different Diversity Technique. In Proceedings of the 2013 IEEE Symposium on Wireless Technology and Applications (ISWTA), Kuching, Malaysia, 22–25 September 2013. [CrossRef]
11. Okoyeigbo, O.; Okokpujie, K.; Noma-Osaghae, E.; Ndujiuba, C.U.; Shobayo, O.; Jeremiah, A. Comparative Study of MIMO-OFDM Channel Estimation in Wireless Systems. *Int. Rev. Model. Simul. (IREMOS)* **2018**, *11*, 158. [CrossRef]
12. Pham, T.; Le-Ngoc, T.; Woodward, G.; Martin, P.A.; Phan, K.T. Equalization for MIMO-OFDM systems with insufficient cyclic prefix. In Proceedings of the IEEE Vehicular Technology Conference, Nanjing, China, 15–18 May 2016. [CrossRef]
13. Hadani, R.; Rakib, S.; Tsatsanis, M.; Monk, A.; Goldsmith, A.J.; Molisch, A.F.; Calderbank, R. Orthogonal Time Frequency Space Modulation. In Proceedings of the 2017 IEEE Wireless Communications and Networking Conference (WCNC), San Francisco, CA, USA, 19–22 March 2017; pp. 1–6. [CrossRef]
14. Raviteja, P.; Member, S.; Phan, K.T.; Hong, Y.; Member, S.; Viterbo, E. Interference Cancellation and Iterative Detection for Orthogonal Time Frequency Space Modulation. *IEEE Trans. Wirel. Commun.* **2018**, *17*, 6501. [CrossRef]
15. Buzzi, S.; Caire, G.; Colavolpe, G.; D'Andrea, C.; Foggi, T.; Piemontese, A.; Ugolini, A. LEO Satellite Diversity in 6G Non-Terrestrial Networks: OFDM vs. OTFS. *IEEE Commun. Lett.* **2023**, *27*, 3013–3017. [CrossRef]
16. Raviteja, P.; Phan, K.T.; Hong, Y.; Viterbo, E. Orthogonal time frequency space (OTFS) modulation based radar system. In Proceedings of the 2019 IEEE Radar Conference (RadarConf), Boston, MA, USA, 16 September 2019. [CrossRef]
17. Hadani, R.; Rakib, S.; Molisch, A.F.; Ibars, C.; Monk, A.; Tsatsanis, M.; Delfeld, J.; Goldsmith, A.; Calderbank, R. Orthogonal Time Frequency Space (OTFS) modulation for millimeter-wave communications systems. In Proceedings of the 2017 IEEE MTT-S International Microwave Symposium (IMS), Honolulu, HI, USA, 4–9 June 2017; pp. 681–683. [CrossRef]
18. Ramachandran, M.K.; Chockalingam, A. MIMO-OTFS in High-Doppler Fading Channels: Signal Detection and Channel Estimation. In Proceedings of the 2018 IEEE Global Communications Conference (GLOBECOM), Abu Dhabi, United Arab Emirates, 9–13 December 2018; pp. 206–212. [CrossRef]
19. Shen, W.; Dai, L.; An, J.; Fan, P.; Heath, R.W. Channel Estimation for Orthogonal Time Frequency Space (OTFS) Massive MIMO. *IEEE Trans. Signal Process.* **2019**, *67*, 4204–4217. [CrossRef]
20. Raviteja, P.; Phan, K.T.; Jin, Q.; Hong, Y.; Viterbo, E. Low-complexity iterative detection for orthogonal time frequency space modulation. In Proceedings of the IEEE Wireless Communications and Networking Conference, WCNC, Barcelona, Spain, 15–18 April 2018; pp. 1–6. [CrossRef]
21. Yuan, W.; Li, S.; Wei, Z.; Cui, Y.; Jiang, J.; Zhang, H.; Fan, P. New delay Doppler communication paradigm in 6G era: A survey of orthogonal time frequency space (OTFS). *China Commun.* **2023**, *20*, 1–25. [CrossRef]
22. Aldababsa, M.; Özyurt, S.; Kurt, G.K.; Kucur, O. A Survey on Orthogonal Time Frequency Space Modulation. *IEEE Open J. Commun. Soc.* **2024**, *5*, 4483–4518. [CrossRef]
23. Xu, C.; Xiang, L.; An, J.; Dong, C.; Sugiura, S.; Maunder, R.G.; Yang, L.-L.; Hanzo, L. OTFS-Aided RIS-Assisted SAGIN Systems Outperform Their OFDM Counterparts in Doubly Selective High-Doppler Scenarios. *IEEE Internet Things J.* **2023**, *10*, 682–703. [CrossRef]
24. Wei, Z.; Li, S.; Yuan, W.; Schober, R.; Caire, G. Orthogonal Time Frequency Space Modulation—Part I: Fundamentals and Challenges Ahead. *IEEE Commun. Lett.* **2023**, *27*, 4–8. [CrossRef]
25. Lampel, F.; Member, S.; Alvarado, A.; Member, S.; Willems, F.M. Orthogonal Time Frequency Space Modulation: A Discrete Zak Transform Approach. *Entropy* **2021**, *24*, 1704. [CrossRef]
26. Mathworks. OTFS Modulation. Available online: https://uk.mathworks.com/help/comm/ug/otfs-modulation.html (accessed on 17 December 2024).